GENE ACTIVATION IN THE MONKEY TEMPORAL CORTEX DURING VISUAL PAIRED ASSOCIATE LEARNING

視覚性対連合学習にともなうサル側頭葉における遺伝子発現

奥野浩行

①

GENE ACTIVATION IN THE MONKEY TEMPORAL CORTEX DURING VISUAL PAIRED ASSOCIATE LEARNING

視覚性対連合学習にともなうサル側頭葉における遺伝子発現

HIROYUKI OKUNO
奥野浩行

TABLE OF CONTENTS

ABSTRACT

In humans and monkeys, memory consists of various components, which were initially revealed through neuropsychological studies of amnesic patients. One of the components, long-term memory regarding facts and events (declarative memory), has been shown to require the integrity of the medial temporal lobe and neocortex. To map the expression pattern of the genes activated during declarative memory formation in primates, I monitored the expression of immediate early genes (IEGs) in the temporal lobe of macaque monkeys. I trained the monkeys to perform visual associative memory tasks, and immunohistochemically analyzed the expression of the protein products of the IEGs. I found that Zif268, a transcription factor regulated by neuronal activity, was accumulated in patches in the perirhinal cortex, especially in area 36, during visual stimulus-stimulus association learning, whereas other transcription factors, c-Fos and JunD, were not. By contrast, such patchy expression of Zif268 in the anterior temporal lobe was not observed during another type of learning, namely, visual discrimination learning. I further quantitatively investigated the *zif*268 mRNA expression levels by a quantitative RT-PCR technique. I found that the *zif*268 mRNA levels in area 36 were significantly higher during stimulus-stimulus association learning compared with those during discrimination learning. Such differences in *zif*268 mRNA expression levels were not observed in the primary visual cortex, temporal association area, or the hippocampus. These results indicate that the neuronal activities during different cognitive tasks could be discriminated by mapping *zif*268 expression, and further suggest that the gene activation in area 36 may contribute to the formation and/or maintenance of long-term memory in primates.

INTRODUCTION

The primate temporal lobe has a crucial role in the cognitive memory and perception, especially, in vision (Mishkin, 1982; Squire and Zola-Morgan, 1991; Miyashita, 1993). Behavioral studies on monkeys have revealed that integrity of the medial temporal lobe and the inferior temporal cortex is essential for visual associative memory (Murray and Mishkin, 1986; Zola-Morgan et al., 1989, 1993). Anatomically, the inferior temporal cortex is located at the final processing stage of the ventral visual stream, which specializes in object/form vision (Van Essen et al., 1992). The perirhinal cortex (i.e., areas 35 and 36), which is a component of the medial temporal lobe memory system, has reciprocal connections with the inferior temporal cortex (Suzuki and Amaral, 1994; Suzuki 1996; Murray and Bussey, 1999). The hippocampal formation receives visual signals from the anterior inferotemporal cortex via the perirhinal cortex and in turn, sends back processed information to it (Squire and Zola-Morgan, 1991; Van Essen et al., 1992; Suzuki, 1996).

Several studies have successfully mapped functional activities in the central nervous system by monitoring the expression of immediate early genes (IEGs), a class of genes that exhibits rapid and transient but protein synthesis-independent increase in transcription (Sheng and Greenberg, 1990; Morgan and Curran, 1991; Hughes and Dragunow, 1995). Electrical stimulation or convulsive compound administration transiently induces the expression of IEGs in the rodent hippocampus and its related cortical areas (Morgan *et al.*, 1987; Saffen *et al.*, 1988; Cole *et al.*, 1990; Hughes *et al.*, 1993). A number of IEGs encode transcription factors such as Fos, Jun and Zif268 and their expression levels have been shown to be either up-regulated or down-regulated in the brain under physiological conditions. Tactile stimulation to whiskers increases the expression of Fos and Zif268 in the rat somatosensory cortex (Mack and Mack, 1992). Mating behavior induces the expression of c-*fos* in the

medial preoptic area in male rats (Baum and Everitt, 1992). In the primary visual cortex, Zif268 expression is increased by exposure to light and decreased by blockage of visual inputs (Worley *et al.*, 1991; Rosen *et al.*, 1992; Chaudhuri *et al.*, 1995). Although the roles of these IEGs are still unclear, some findings imply that these IEGs, especially *zif*268, may be involved in genomic responses in neural processes related to learning and memory (Alberini *et al.*, 1994; O'Donovan *et al.*, 1999). The induction of *zif*268 in the dentate gyrus is closely correlated with the induction of long-term potentiation (LTP), which is a candidate for the cellular basis of associative memory (Abraham *et al.*, 1993; Worley *et al.*, 1993). In songbirds, *zif*268 expression is strongly induced in specific regions of the auditory telencephalon (medial caudal neostriatum) when the birds hear a song sung by one of their own species, but induced only slightly when the birds hear songs sung by other species (Mello *et al.*, 1992). Furthermore, the song-induced *zif*268 expression in songbirds increases under conditions of associative learning between song and shock (Jarvis *et al.*, 1995).

The intracellular mechanisms of IEG induction have been investigated extensively in neuronal cells (Ginty *et al.*, 1992; Sakamoto *et al.*, 1994; McMahon and Monroe, 1995; Kumahara *et al.*, 1999). The promoter sequence of *zif*268 gene has several unique regulatory elements including cyclic-AMP responsive elements (CREs) and serum-responsive elements (SREs) (Lemaire *et al.*, 1988; Changelian, *et al.*, 1989; Christy and Nathans, 1989). Increase in intracellular cAMP or Ca^{2+} levels causes activation of intracellular kinases such as protein kinase A (PKA) or calcium/calmodulin-dependent protein kinase (CaMK), and these kinases then phosphorylate CRE-binding proteins (CREBs): the phosphorylated CREBs can bind to the CRE sequneces and trigger IEG expression (Vaccarino *et al.*, 1993; Lerea *et al.*, 1992; Bito *et al.*, 1996). It is known that the SRE is a major regulatory element of the promoter that is activated through the ras/ERK pathway of the mitogen-activated protein kinase pathways

(Hill and Treisman, 1995; Marshall, 1995). Indeed, activation of these intracellular signaling pathways effectively induces *zif*268 gene expression (Ginty *et al.*, 1991; Cole *et al.*, 1989, 1992; McMahon and Monroe, 1995; Ebihara and Saffen, 1997).

In the present study, I attempted to investigate brain areas in which IEGs are expressed during visual long-term memory formation in primates. I trained monkeys to learn two different cognitive memory tasks, a visual pair-association task and a visual discrimination task. The visual pair-association task is a modified form of the verbal paired associate paradigm that is clinically used to assess specific impairment of long-term memory regarding facts and events, that is declarative memory, in humans (Wechsler, 1987; Squire and Zola-Morgan, 1991). This task required the monkeys to memorize visual stimulus-stimulus associations (Sakai and Miyashita, 1991; Higuchi and Miyashita, 1996; Hasegawa *et al.*, 1998). The other task, the visual discrimination task, required them to memorize stimulus-reward associations (Iwai and Mishkin, 1969; Murray and Mishkin, 1986). The types of learning required in these tasks are different since they are affected by lesions in different brain areas (Iwai and Mishkin, 1969; Murray *et al.*, 1993; Suzuki *et al.*, 1993). This finding prompted us to test whether the different memory systems could be discriminated by mapping the expression patterns of IEGs. In the present study, I investigated IEG expression by two different methods. I first immunohistochemically examined the distribution of Zif268 protein in the monkey temporal cortex. I found that the pattern of Zif268 expression in the anterior temporal cortex during visual paired associate learning differed from that during visual discrimination learning. I next quantitatively examined *zif*268 mRNA expression levels by a quantitative RT-PCR method, and found that, in the perirhinal cortex, the *zif*268 mRNA levels during paired associate learning were significantly higher than those during discrimination learning.

MATERIALS AND METHODS

Subjects

The subjects were male macaque monkeys (*Macaca fuscata*), all weighing between 7.0 and 9.6 kg at the time of perfusion. For immunohistochemical study, three monkeys were trained to learn a visual pair-association task and other three monkeys were trained to learn a visual discrimination task as described below. For RNA quantification study, five monkeys were trained to learn both of the visual pair-association and discrimination tasks. All animal experiments were carried out in accordance with the regulations of the University of Tokyo School of Medicine, the Guide for the Care and Use of Laboratory Animals (National Academy Press, 1996) and Preparation and Maintenance of Higher Mammals during Neuroscience Experiments (NIH Publication, 1991).

Apparatus and Stimuli

The training apparatus for the monkeys was a computer-controlled test system that consisted of a soundproof room, a video monitor with a touch panel and an automatic juice supplier (Fig. 1). Fourier descriptors were generated according to the algorithm described by Zahn (Zahn and Roskies, 1972; Sakai and Miyashita, 1991). They were randomly sorted into pairs of geometrically distinct patterns. Several sets of the 12 pairs of the Fourier descriptors were used as visual stimulus sets (Fig. 2A, B) in both pair-association and visual discrimination tasks. The size of each visual stimulus presented on the video monitor was approximately 6 cm wide by 6 cm long. The distance from the monkeys to the video monitor and the touch panel was set at 17 cm.

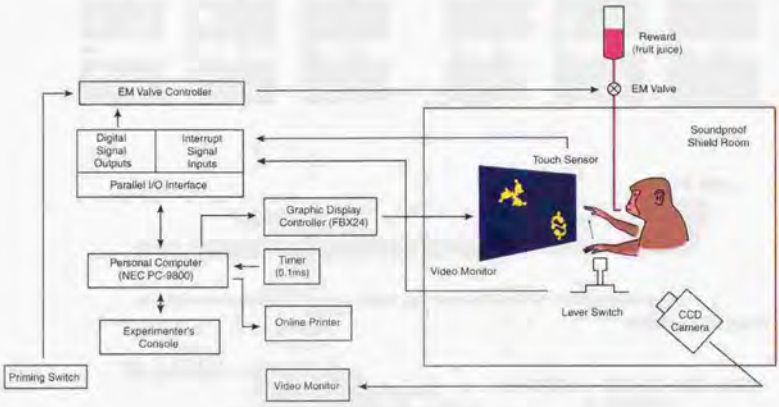

Fig. 1. Experimental set-up for monkey behavioral tasks. The direction of information flow is indicated by arrows connecting each device shown in a box. A custom-made program for behavioral tasks run on a personal computer controlled initiation of a task trial, visual stimulus presentation, and supply of juice reward.

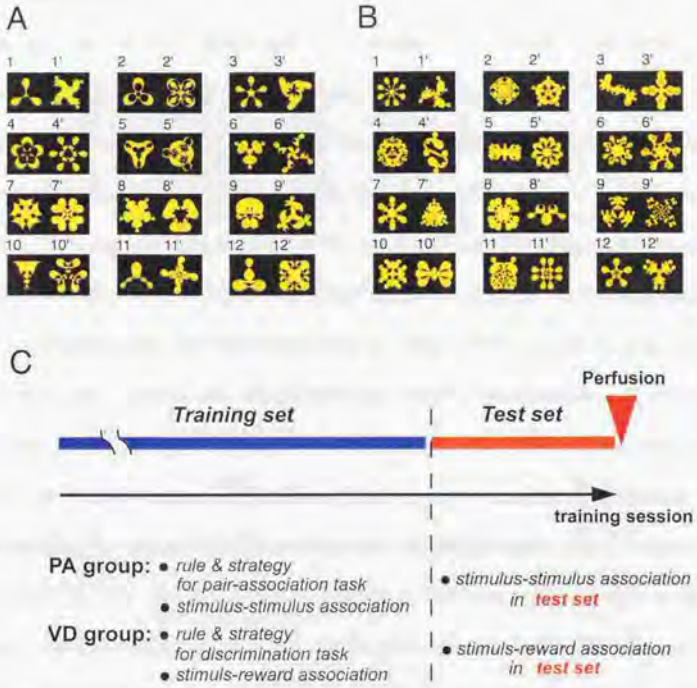

Fig. 2 Experimental schedule for visual long-term memory in monkeys. (A) A set of stimulus pictures used for the initial training phase of the visual memory tasks (*training set*). The pictures were generated using a computer, randomly sorted into pairs, and used as a stimulus set in the visual pair-association (PA) task and the visual discrimination (VD) task. (B) Another set of 24 pictures was also generated using the same algorithm as the *training set*, and used for the second training phase (*test set*). (C) Training schedule of visual long-term memory tasks. The monkeys were first trained to perform the tasks with the *training set*. After the monkeys had learned the task "rule" with the training set, a new set of stimuli, that is *test set*, was introduced. The monkeys executed approximately 600 trials in a training session per day in both the pair-association task and the discrimination task after the introduction of the *test set*. On the eighth to tenth day with the test set, the monkeys learning pair-association task were anesthetized and immediately perfused following that day's training session. The monkeys learning discrimination task were perfused after the training session on the fifth or sixth day.

Visual memory tasks

The monkeys were trained to learn a visual pair-association task (Sakai and Miyashita, 1991; Murray *et al.*, 1993; Higuchi and Miyashita, 1996; Hasegawa *et al.*, 1998) or visual discrimination task (Iwai and Mishkin, 1969; Murray and Mishkin, 1986). The procedure of the visual pair-association task was essentially the same as described previously (Sakai and Miyashita, 1991; Higuchi and Miyashita, 1996) except that monkeys sequentially learned the *training set* and the *test set* of paired associates in this study (Fig. 2). In this task, each trial started with a green square for fixation that was presented on the center of the video monitor for 0.5 s (Fig. 3A). Then, the cue stimulus that was randomly selected from a set of stimulus pictures was presented at the same position for 1 s. After a delay of 4 s, choice stimuli were presented randomly in two of four positions (arranged in two rows of two columns). The choice stimuli were consisted of the paired associate of the cue stimulus and a stimulus from another pair (Fig. 3B). The monkeys were required to touch the paired associate of the cue stimulus to obtain fruit juice as a reward. In the other task, the visual discrimination task, monkeys sequentially learned the *training* and *test* sets of visual stimuli as in the visual pair-association task (Fig. 2). Each trial of this task started with the green square and then choice stimuli were presented randomly in two of four positions of the video monitor (Fig. 4A). The choice stimuli were consisted of a pair of pictures that were fixed as a rewarded stimulus and a non-rewarded stimulus (Fig. 4B). The choice pair was randomly selected from a set of 12 pairs of stimulus pictures. The monkeys were required to touch the rewarded stimulus to obtain fruit juice. The amount of the juice reward was altered to control monkey's motivational and attentive levels.

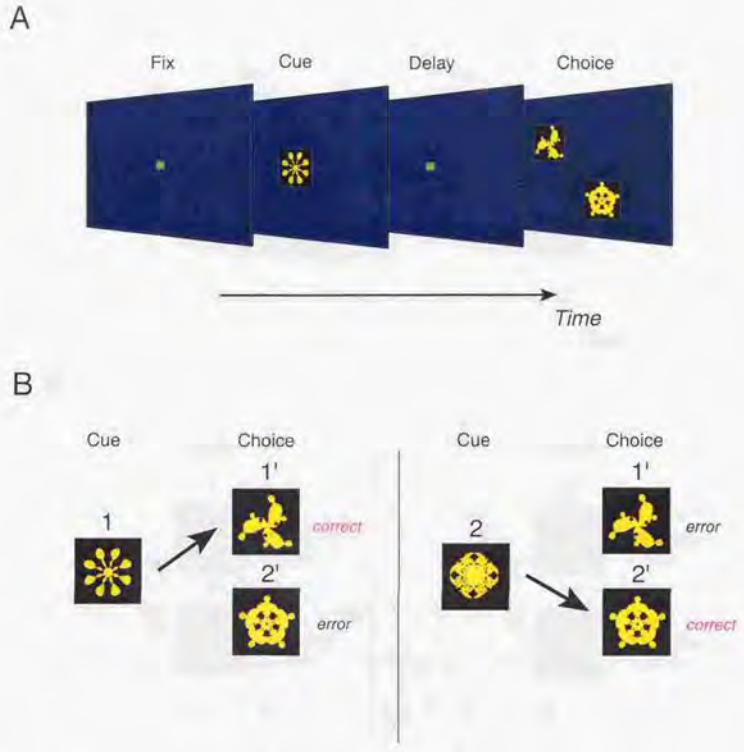

Fig. 3. Visual pair-association task. (A) Sequence of events in a trial of the visual pair-association task. A trial started with a green square for fixation presented in the center of a video monitor. A cue stimulus was then presented in the center and, after a delay, choice stimuli were presented randomly in two of four positions. (B) Role of stimulus pairs in the pair-association task. A stimulus pair was used as paired associates in this task. The choice stimuli consisted of the paired associate of the cue stimulus and a stimulus from another pair. The monkeys were required to touch the paired associate of the cue stimulus to obtain fruit juice as a reward.

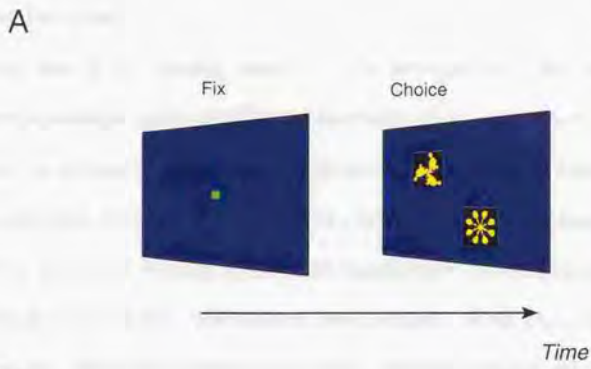

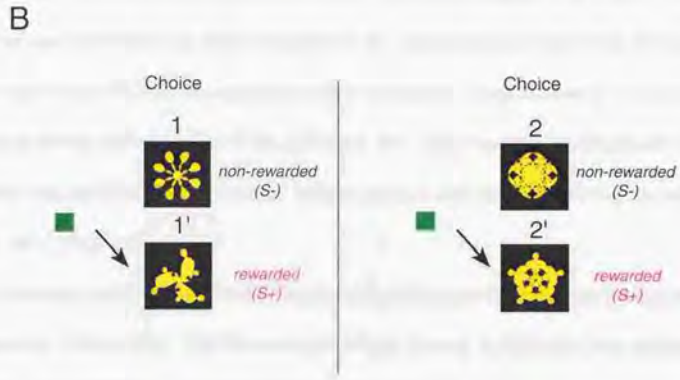

Fig. 4. Visual discrimination task. (A) Sequence of events in a trial of the visual discrimination task. A trial started with the green square and then choice stimuli were presented randomly in two of four positions of the video monitor. (B) Role of stimulus pairs in the visual discrimination task. The choice stimuli consisted of a pair of pictures that were fixed as a rewarded stimulus (S+) and a non-rewarded stimulus (S-). The monkeys were required to touch the rewarded stimulus to obtain fruit juice.

Immunohistochemistry

After the end of the training session on the perfusion day, the monkeys for the immunohistochemical experiments were immediately given an overdose of pentobarbital (>40 mg/kg) and then perfused transcardially as described previously (Okuno *et al.*, 1995, 1997). Essentially, the perfusion was initiated with 0.9% NaCl at room temperature for 2 min at a rate of 300 ml/min, followed by 4% paraformaldehyde/0.1 M phosphate buffer (pH7.4) at same rate for 10 min at 4°C. The perfusion was continued with the same solution for 50 min at 100 ml/min. During the perfusion, the monkey's head was wrapped with crushed ice. The brain was removed from the skull, blocked in the coronal plane, immersed in the same fixative for 6 h at 4°C, and cryoprotected with increasing concentrations (5% to 20%) of sucrose/phosphate-buffered saline (PBS; pH7.4) at 4°C. The brain blocks were frozen in dry-ice powder and sections (32μm) were cut using a cryostat. All sections were kept in sampling tubes at -80°C until use.

The monkey brain sections were stained immunohistochemically as described previously (Okuno *et al.*, 1995, 1997). The frozen sections were thawed in PBS, and then incubated in PBS containing 0.3% H_2O_2 for 30 min at room temperature to reduce endogenous peroxidase activity. After washing with PBS (room temperature, 15 min with three changes), the sections were incubated with blocking solution containing PBS plus 10% normal goat serum and 0.3% Triton X-100 for 60 min at room temperature, followed by incubation with blocking buffer containing the primary antibody (see below) at 4°C for 24 h. The sections were washed with PBS, then incubated with blocking buffer containing horseradish peroxidase (HRP)-conjugated goat anti-rabbit IgG antibody (Jackson ImmunoResearch; cat. no. 111-035-003; diluted 1:400) at room temperature for 2 h. After washing with PBS and Tris-buffered saline (50 mM Tris-Cl, 150 mM NaCl; pH7.4), the sections were reacted with

coloring solution (0.2 mg/ml 3,3'-diaminobenzidine tetrahydrochloride, 0.05% H_2O_2, 0.08% nickel chloride in 50 mM Tris-Cl, pH7.4) for 10 min at room temperature.

For cytoarchitecture identification, sections adjacent to immunostained sections were stained by cresyl violet. The nomenclature and anatomical criteria for delimitation of the cortical areas in this study were based on those used previously to describe the monkey temporal lobe (Amaral *et al.*, 1987; Horel *et al.*, 1987).

Antibodies

All primary antibodies used in this study were rabbit polyclonal antibodies. An anti-Zif268 antibody was raised against a synthetic oligopeptide (19 amino acid residues) corresponding to the carboxy terminus of Zif268 (a gift from Dr. D. W. Saffen of the Department of Neurochemistry, University of Tokyo School of Medicine). The antigenic sequence is evolutionary conserved among various species, including rodents, monkeys and humans (Fig. 6). The specificity and reactivity of the anti-Zif268 antibody to monkey *zif*268 gene product were determined previously (Okuno *et al.*, 1995): the anti-Zif268 antibody specifically recognized an 86 kDa protein in the nuclear extracts from monkey cerebral cortex in immunoprecipitation experiments (see also Results). The molecular weight of the protein was nearly identical to that of Zif268 in mice, rats and humans. For antigen-preabsorption experiments, the anti-Zif268 antibody was incubated with peptide antigen (10 ng/ml) for 3 h at 4°C before incubation with the sections. An anti-c-Fos antibody was purchased from Oncogene Science Inc. (cat. no. PC05). The antigen for the anti-c-Fos antibody was a peptide corresponding to residues 4 to 17 of human c-*fos* gene product. This antibody recognizes both rodent and human c-Fos and does not react with other Fos family proteins. An anti-JunD antibody was purchased from Santa Cruz Biotechnology (cat. no. sc-74). The antigen

for the anti-JunD antibody was a peptide corresponding to residues 329 to 341 of mouse *jun*D gene product. This antibody also recognizes both rodent and human JunD but does not cross-react with other Jun family proteins. For the double-labeling study, anti-PKC antibody (Santa Cruz Biotech. cat. no. sc-77) was used for the second immunostaining after the initial staining with the anti-Zif268 antibody. The primary antibodies were diluted as follows: anti-Zif268, 1:2000; anti-c-Fos, 1:500; anti-JunD, 1:1000; anti-PKC, 1:1000.

Image analysis

To visualize the spatial distribution of Zif268, an image (resolution, 4096 × 4096 pixels for 1.57×10^{-2} mm^2) was obtained from each of the serial Zif268-immunostained sections at 0.5 mm intervals (20 sections for each subject) by a CCD camera attached to a microscope, and optical density (OD) was measured in each pixel (pixel OD) using a computer-aided image analyzer (IBAS-V2.0, Zeiss). I evaluated the expression levels by OD measurement (Hughes *et al.*, 1993; Abraham *et al.*, 1994) rather than by cell counting because of variability of Zif268 expression levels in individual neurons. This high resolution image analysis, in which the pixel size was much smaller than the size of neuronal nuclei, enables detailed evaluation of Zif268 expression levels.

The cortical area (layers II to VI) in each section was segmented into 0.5 mm wide strips radially from the white matter to the cortical layer I (see Fig. 9, left). In each segment, the pixel ODs could be classified into two groups, pixel ODs originating from Zif268-immunostaining reaction products in the nuclei and those originating from background staining. The pixel ODs originating from background staining were estimated by fitting a Gaussian distribution to the lowest peak of the distribution of pixel OD using the maximum likelihood method. The density of Zif268-immunostaining reaction products in each segment

was calculated by summing all pixel ODs after subtracting ODs originating from background staining and by normalizing to the area of the segment. The segments were reconstructed into a two-dimensional unfolded map (see Fig. 9) by essentially the same procedure as described by Van Essen and Maunsell (1980). The density of the immunostaining reaction products was indicated on the unfolded map in pseudocolor representation.

Western blotting analysis

Monkey cell line CV-1 cells (provided by RIKEN Cell Bank) were kept in Dulbecco's minimal essential medium with 0.2% fetal bovine serum (FBS) for 16 h, and were harvested at 0 min, 60 min or 360 min after stimulation with 10% FBS. The cells were homogenized and nuclear extracts were prepared as described previously (Okuno *et al.*, 1991). The protein concentration of the samples was assayed using the Bio-Rad protein assay kit (Bio-Rad). The nuclear extracts (25 μg) were resolved on a SDS-polyacrylamide gel and transferred to a PVDF membrane (Millipore, Immobilon P). The membrane was treated with the blocking buffer followed by incubation with the anti-Zif268 antibody, washed with PBS containing 0.3% Tween-20, and then reacted with HRP-conjugated anti-rabbit IgG antibody as described previously (Okuno *et al.*, 1993). For detecting HRP activity, the ECL Western Blotting Detection System (Amersham) was used according to the manufacturer's instructions.

PCR cloning of monkey zif268 gene

Partial cDNA fragments of monkey *zif*268 were isolated and sequenced to investigate the nucleotide and predicted amino-acid sequences of the monkey *zif*268 gene. Total RNA was extracted from the monkey cerebral cortex by the guanidium-thiocyanate (GTC)/CsTFA method as described previously (Okuno *et al.*, 1999). Briefly, the monkey brain tissues were

homogenized in a GTC solution, loaded on a cushion of CsTFA/EDTA solution, ultra-centrifuged, and purified by phenol and by phenol/chloroform extraction. The total RNA was then reverse-transcribed and the first strand cDNA was amplified by PCR as described below. For the PCR amplification, synthetic oligonucleotide primers were generated in accordance with nucleotide sequences conserved between humans and rodents: the forward primer (5'-ATCAAACCCAGCCGCATGCGCAAGT-3') contained 25 bases corresponding to bases 1216-1240 of a human *zif*268 cDNA (GenBank X52541) and the reverse primer (5'-CTGTTTCAGGCAGCTGAATC-3') contained 21 bases complementary to bases 2111-2131 of the human *zif*268 gene. The PCR amplified fragments were purified and subcloned into a plasmid vector, pBluescript II SK+. The PCR-generated clones were sequenced by the dideoxy chain termination method. Glucose-6-phosphate dehydrogenase (G6PD) cDNA fragments of the macaque monkey were also amplified, subcloned and sequenced for an endogenous internal control in a quantitative RT-PCR method described below.

RT-PCR coamplification of zif268 mRNA with endogenous internal standard mRNA

Primers. The primers specific to each mRNA for monkey *zif*268 and G6PD were generated for reverse-transcription (RT)-PCR amplification. All primer sequences were designed faithfully based on sequences of the macaque monkey *zif*268 and G6PD clones described above to avoid generating mismatched primers. The sequences of the primer pairs for each gene are listed in the following table. The locations of fragments of *zif*268 amplified using the primer pairs are schematically represented in figure 6. The primers for *zif*268 were designed to amplify a 250-bp fragment and the primers for the G6PD gene were designed to amplify a 211-bp fragment.

Primers for RT-PCR quantification

Gene	Oligonucleotide sequence
*zif*268	
Upper primer:	5'-CGGTTACTACCTCTTATCCATC-3'
Reverse primer:	5'-GAAAATGTTGCTGTCATGTC-3'
G6PD	
Upper primer:	5'-AAGCCCGCCTCCACCAACTC-3'
Reverse primer:	5'-CCACATAGAGGACGACGGCT-3'

The upper primer for *zif*268 contained 22 bases corresponding to bases 1628-1649 of the human *zif*268 cDNA (GenBank X52541) and the reverse primer contained 20 bases complementary to bases 1858-1877 of the human *zif*268 gene. The upper primer for G6PD contained 20 bases corresponding to bases 364-383 of a human G6PD cDNA (GenBank M12996) and the reverse primer contained 20 bases complementary to bases 555-574 of the human G6PD gene.

Reverse-transcription. The RNA samples were diluted to the same concentration, reverse-transcribed to cDNAs using random 9 mers as primers, and used as initial templates for PCR amplification as described previously (Okuno *et al.*, 1999; Tokuyama *et al.*, 1998). For each sample, 500 ng of total RNA were reverse-transcribed in 20μl of the reverse-transcription mixture (10 mM Tris-Cl (pH 8.3), 50 mM KCl, 5 mM $MgCl_2$, 1 mM of each dNTP, 2.5 μM of random 9 mers, 0.5 U/μl of human pancreas ribonuclease inhibitor and 1 U/μl of avian myeloblastosis virus reverse transcriptase; Takara Biomedicals, Kyoto, Japan) by incubating at the mixture 30 °C for 15 minutes followed by incubation at 42 °C for 30 minutes. The reaction was terminated by heating the mixture at 95 °C for 5 minutes and immediately cooling it at 4 °C.

PCR amplification. The reverse-transcribed mRNAs were analyzed using a PCR coamplification with endogenous internal standard method (Gause and Adamovicz, 1995). The PCR was performed in a reaction volume of 10 µl containing 2.0 µl of RT reaction products, 10 mM Tris-Cl (pH 8.3), 50 mM KCl, 2.5 mM $MgCl_2$, 0.2 µM of each primer for both target and endogenous internal standard genes (see below), 0.2 mM dNTPs, 5 µCi α-^{32}P-dCTP (3000 mCi/mol, Amersham) and 0.25 U *Taq* polymerase (Takara Biomedicals). The endogenous internal standard gene was simultaneously amplified with a target gene in the same reaction tubes to circumvent tube-to-tube variations (Chelly *et al.*, 1988; Pang *et al.*, 1990). In the present study, G6PD mRNA was used as an internal standard since this gene is ubiquitously and constitutively expressed throughout the brain at relatively constant levels (Okuno *et al.*, 1999). The PCR was carried out as follows. An initial denaturation step was for 1 minute at 94.0 °C, and each cycle consisted of three steps: a 30-second denaturation step at 94.0 °C, a 30-second annealing step at 57.0 °C and a 90-second extension step at 72.0 °C. The amplified PCR products were separated on 6% polyacrylamide gels, which were dried by vacuum suction, and detected by autoradiography. The RT-PCR products were quantitated using radioisotope image analyzers, BAS2000 (FUJI, Japan). In each quantification experiment, I measured the radioactivity incorporated in fragments representing the *zif*268 and the internal standard G6PD over two PCR cycles before the plateau effect occurred, and confirmed that both fragments were amplified exponentially with the same efficiency. For normalization, the radioactivity incorporated in the *zif*268 fragments was divided by that incorporated in the internal standard fragments in each PCR cycle. The *zif*268 expression levels for each brain area were averaged across the PCR cycles and defined as the relative mRNA levels.

Tissue preparation for RNA quantification

For the RNA quantification experiments, I prepared split-brain animals. Five macaque monkeys were subjected to transection of forebrain commissures, the corpus callosum and the anterior commissure. By this transection, information transfer between the two hemispheres was blocked (Hasegawa *et al.*, 1998). I then trained each monkey to perform both of the visual pair-association and discrimination tasks. Procedures for these visual tasks were essentially the same as the case in the immunohistochemical experiments, except that, in the quantification experiment, the monkeys must maintain fixation during presentation of the visual stimuli. In the task trials, visual stimuli were presented in one visual hemifield for the pair-association task and the other hemifield for the discrimination task. This stimulus configuration enables each monkey to perform separately the visual pair-association task using one hemisphere and discrimination task using the other. Eye position was monitored with the scleral search coil method (Hasegawa *et al.*, 1998). Before the monkeys' performance reached a plateau level, their brains were removed as described before except that the animals were not perfused with the fixative.

In each animal, four cortical areas (primary visual area V1, visual association area TE, area 36 in the perirhinal cortex and the hippocampus) were separately excised on the basis of cortical landmarks, such as sulci and gyri, and processed for RNA extraction (Okuno *et al.*, 1999). The landmarks for the excision are followings. The primary visual cortex (V1) was excised from the occipital surface, and from the dorsal and ventral banks of the calcarine sulcus. The border between V1 and neighboring area V2 could be visually identified without histochemical or immunohistochemical staining by the existence of a fiber band extended parallel to the pial surface in the middle of the cortical layer of V1 (Lund, 1988; Okuno *et al.*, 1997) . Since the medial border of TE could not be reliably identified without

cytoarchitectonical and immunohistochemical staining, a conservative putative border was set at the fundus of the anterior middle temporal sulcus (AMTS) at the rostral level and at the fundus of the OTS at the caudal level (Fig. 1D)(Iwai *et al.*, 1987). The anterior end of the posterior middle temporal sulcus (PMTS) was regarded as a conservative putative border between TE and TEO. Area 36 of the perirhinal cortex is located laterally to area 35 and medially to TE. Since the border between areas 36 and TE could not be reliably identified without cytoarchitectonical and immunohistochemical staining as described above, a conservative putative lateral border of area 36 was set at a position one-third to one-half the distance from the medial lip of the AMTS toward the lateral lip of the rhinal sulcus (RS) (Suzuki and Amaral, 1994). In two monkeys, the rostral part of area 36 was used for the RNA extraction on the based of the results form the immunohistochemical experiments (Fig. 10). A conservative medial border of area 36 was set at the lateral/ventral lip of the RS. The hippocampus, including the dentate gyrus, was excised from the medial temporal lobe by incision at the subicular region. In the present study, as described above, some excised areas might not contain the whole of target area because I wanted to isolate target areas without contamination by other areas.

RESULTS

Visual paired associate learning and visual discrimination learning

I trained monkeys to learn a visual pair-association (Sakai and Miyashita, 1991; Murray *et al.*, 1993; Higuchi and Miyashita, 1996) or visual discrimination (Iwai and Mishkin, 1969; Murray and Mishkin, 1986) task using several sets of computer-generated pictures (Fig. 2). To investigate formation of associative memory of the visual stimuli but not skill-based or habit-like memory incidental to the task paradigm, I first trained the monkeys to learn a "rule" or "strategy" of the tasks, which is considered to be related to the latter memory classes, using a set of 24 pictures (*training set*). In the visual pair-association task, the monkeys were required to recognize a cue stimulus, recall its paired associate and correctly touch the paired associate on a monitor to obtain fruit juice as a reward (Fig. 3). In the visual discrimination task, the monkeys were required to discriminate a rewarded stimulus from a non-rewarded stimulus and touch the rewarded stimulus to obtain the reward (Fig. 4). After the monkeys' performance reached a plateau level with the *training set*, a new stimulus set (*test set*) was introduced to access formation of the new associative memory of the new visual stimuli (Fig. 2). The monkeys' performance was at a chance level (i.e., 50 % correct responses) in the first session with the *test set*, then improved gradually in subsequent test sessions (Fig. 5). To examine gene activation during the learning of the *test set*, the monkeys were perfused immediately after the completion of the test session before the performance reached a plateau phase (Figs. 2 and 5). The monkeys in the both groups were exposed to equivalent number of visual stimuli (pair-association, 684±102 stimuli per hour; discrimination, 664±72) during 2 hours before the perfusion.

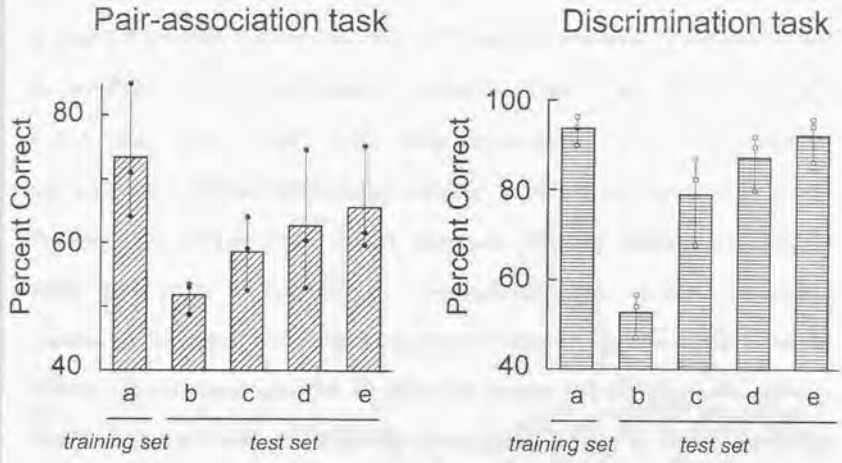

Fig. 5. Monkeys' performance in the pair-association task and the discrimination task. Monkeys learned the pair-association task or the visual discrimination task with a *training set* of stimulus pictures, and then with a new set of pictures (*test set*). (a) the mean percent correct of the session with the training set immediately before the introduction of the *test set*; (b) that of the first session with the *test set*; (c) That of the second session with the *test set*; (d) that of the session with the *test set* in one day before perfusion; (e) that of the session with the *test set* immediately before perfusion. Filled (left panel) and open (right panel) circles indicate the mean percent correct of individual monkeys in the visual pair-association and discrimination tasks, respectively.

Detection of monkey Zif268

To detect inducible transcription factors encoded by IEGs at single-cell resolution, I stained serial coronal sections of the anterior temporal lobe of the monkeys immunohistochemically as described previously (Okuno *et al.*, 1995, 1997). In a previous study, in which I examined the specificity of an anti-Zif268 antibody, I demonstrated that monkey Zif268 is an 86 kDa protein which is present at high levels in nuclei and is expressed in the cerebrum but not in the cerebellum, by immunoprecipitation experiments (see Fig. 1 in Okuno *et al.*, 1995). In this study, I first examined peptide sequence of monkey Zif268 by sequencing PCR-generated *zif*268 clones of the macaque monkey. The peptide sequence, including an antigenic sequence of the anti-Zif268 antibody, is evolutionarily conserved well among various species (Fig. 6). I then analyzed expression of Zif268 in the monkey cells after serum stimulation by Western blotting to examine the inducibility of monkey Zif268 (Fig. 7). With the anti-Zif268 antibody, a band corresponding to an 86 kDa protein was transiently detected 1 h after the stimulation (Fig. 7, lane 2). This band was not detected with the antigen-preabsorbed antibody (Fig. 7, lane 4), indicating that the band represents induced monkey Zif268.

Intense immunoreactivity was observed in the monkey brain sections stained with the anti-Zif268 antibody. In each cell, the Zif268-immunoreactivity was accumulated in round and its size was larger than Nissl-stained glial cells but smaller than Nissl-stained neuronal somata (Fig. 7B, C). In the sections subjected to double labeling with the anti-Zif268 and anti-PKC antibodies, Zif268-immunoreactivity was localized in the nuclei whereas PKC-immunoreactivity was observed in the cytosolic compartment (data not shown). The immunoreactivity was Zif268 specific because the antigen-preabsorbed antibody failed to stain any cells (Fig. 7D). These results indicate that Zif268-immunoreactivity is localized in the nuclei of neurons and absent in glial cells as shown previously (Herdegen *et al.*, 1993;

Okuno *et al.*, 1995), implying that Zif268 acts as a neuron-specific transcription factor in the brain.

A

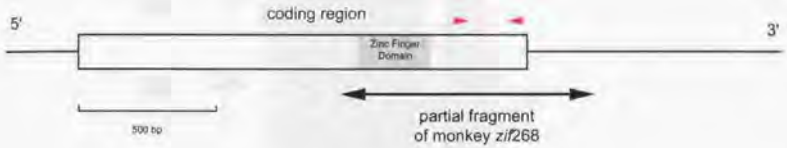

B

```
Monkey     ________S RMRKYPNRPS KTPPHERPYA CPVESCDRRF SRSDELTRHI RIHTGQKPFQ CRICMRNFSR SDHLTTHIRT
Human      ________S RMRKYPNRPS KTPPHERPYA CPVESCDRRF SRSDELTRHI RIHTGQKPFQ CRICMRNFSR SDHLTTHIRT
Rat        ________S RMRKYPNRPS KTPPHERPYA CPVESCDRRF SRSDELTRHI RIHTGQKPFQ CRICMRNFSR SDHLTTHIRT
Mouse      ________S RMRKYPNRPS KTPPHERPYA CPVESCDRRF SRSDELTRHI RIHTGQKPFQ CRICMRNFSR SDHLTTHIRT

Monkey     HTGEKPFACD ICGRKFARSD ERKRHTKIHL RQKDKKADKS VVASSATSSL SSYPSPVATS YPSPVTTSYP SPATTSYPSP
Human      HTGEKPFACD ICGRKFARSD ERKRHTKIHL RQKDKKADKS VVASSATSSL SSYPSPVATS YPSPVTTSYP SPATTSYPSP
Rat        HTGEKPFACD ICGRKFARSD ERKRHTKIHL RQKDKKADKS VVASSAASSL SSYPSPVA.. ......TSYP SPATTSFPSP
Mouse      HTGEKPFACD ICGRKFARSD ERKRHTKIHL RQKDKKADKS VVASPAASSL SSYPSPVA.. ......TSYP SPATTSFPSP

Monkey     VPTSFSSPGS STYPSPVHSG FPSPSVATTY SSVPPAFPAQ VSSFPSSAVT NSFSASTGLS DMTATFSPRT IEIC*
Human      VPTSFSSPGS STYPSPVHSG FPSPSVATTY SSVPPAFPAQ VSSFPSSAVT NSFSASTGLS DMTATFSPRT IEIC*
Rat        VPTSYSSPGS STYPSPAHSG FPSPSVATTY ASVPPAFPAQ VSTFQSAGVS NSFSTSTGLS DMTATFSPRT IEIC*
Mouse      VPTSYSSPGS STYPSPAHSG FPSPSVATTF ASVPPAFPTQ VSSFPSAGVS SSFSTSTGLS DMTATFSPRT IEIC*
```

Fig. 6. PCR cloning of monkey *zif*268. (A) Putative structure of monkey *zif*268 mRNA. A region underlined by an arrow indicates a portion analyzed by PCR cloning. Small red arrowheads indicate the location of primers used for RT-PCR quantification experiments. (B) Comparison of amino acid sequences of Zif268 across monkeys, humans and rodents. The sequences are in the one-letter code were aligned by the Bestfit program of the UWGCG package. The amino acids that differ from the human sequence are denoted in blue. Letters in red indicate an antigenic sequence of the anti-Zif268 antibody used in this study. The shaded area represents the DNA binding domain of Zif268 and asterisks indicate the termination of the open-reading frame.

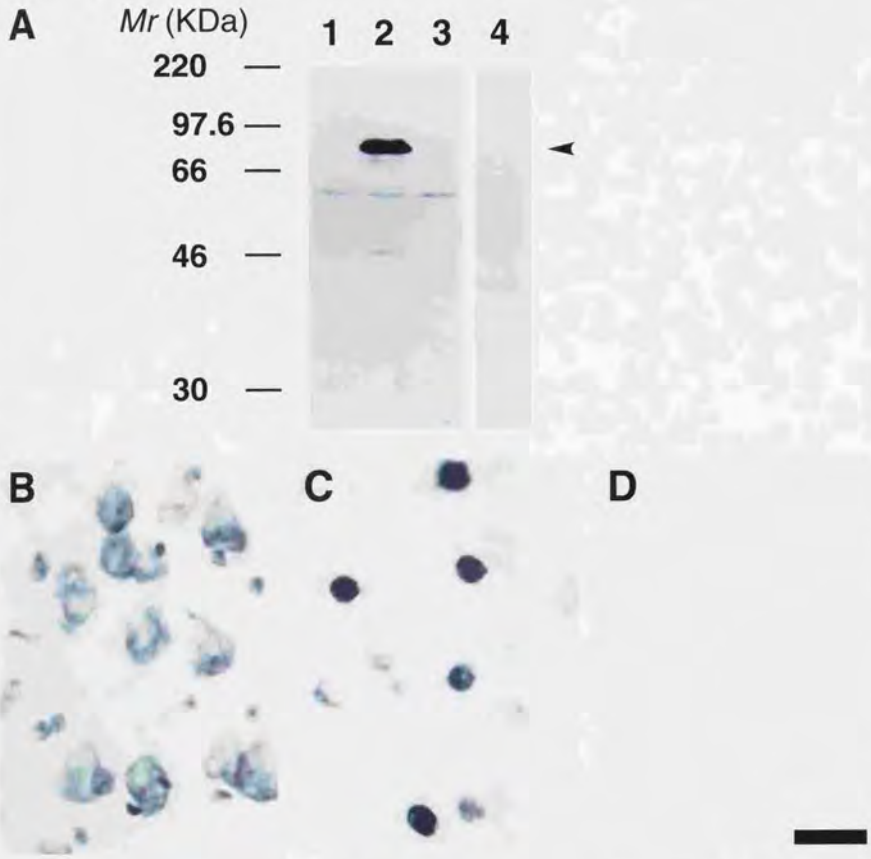

Figure 7

Legends

Fig. 7. Immunodetection of monkey Zif268. (A) Inducibility of monkey Zif268. Serum-starved monkey cells (CV-1) were stimulated with fetal bovine serum, and their nuclear extracts were isolated at 0 (lane 1), 60 (lanes 2 and 4) or 360 (lane 3) min after the stimulation. The nuclear extracts were analyzed by Western blotting with the anti-Zif268 antibody (lane 1-3) or antigen-preabsorbed antibody (lane 4). An arrowhead indicates the band corresponding to induced monkey Zif268. Positions of molecular markers are shown at the left. (B-D) Localization of Zif268-immunoreactivity in the monkey neurons. Serial sections of the monkey temporal lobe were stained with cresyl violet (B), the anti-Zif268 antibody (C) or the antigen-preabsorbed antibody (D). Note that no cells were stained with the antigen-absorbed antibody. Scale bar, 25μm.

Expression of Zif268 in the monkey inferior temporal gyrus

I first examined expression of Zif268 in the anterior temporal cortex of the monkeys during visual paired associate learning and visual discrimination learning. During visual paired associate learning, intensely Zif268-immunopositive neurons were observed in the inferior temporal gyrus, the area that lies between the rhinal sulcus and the anterior middle temporal sulcus (Fig. 8A, B). Figure 3C shows a representative section; the intensely Zif268-immunopositive neurons were accumulated in patches in the ventral surface of the inferior temporal gyrus rather than in the banks of the rhinal sulcus or the anterior middle temporal sulcus. The patches were centered in layer IV and spread into both superficial (II/III) and deep (V and VI) layers (Fig. 8D). The patchy pattern was found in several consecutive sections and was specific to Zif268 since other IEG products did not show such patterns in the adjacent sections (see below). This Zif268-immunostained pattern was observed in all monkeys with paired associate learning. By contrast, during visual discrimination learning, Zif268-immunopositive neurons were found mainly in layer IV and did not show patchy distribution in the inferior temporal gyrus (Fig. 8E, F).

The distribution of Zif268 expression in the monkey temporal cortex was visualized by the image analysis (see Methods) and displayed on a two-dimensional unfolded map (Figs. 9 and 10). In each monkey with visual paired associate learning, Zif268 was expressed at high levels in a strip parallel to the rhinal sulcus in an anterior-posterior axis, particularly at several spots in this strip (PA1-PA3). Zif268 was expressed at relatively low levels and was distributed more homogeneously in the monkeys with visual discrimination learning (VD1-VD3). The inferior temporal gyrus is composed of three cytoarchitectonically and connectionally distinct areas (area 35, area 36 and ventral part of area TE) (Martin-Elkins and Horel, 1992; Suzuki and Amaral, 1994). The expression of Zif268 in the monkeys during

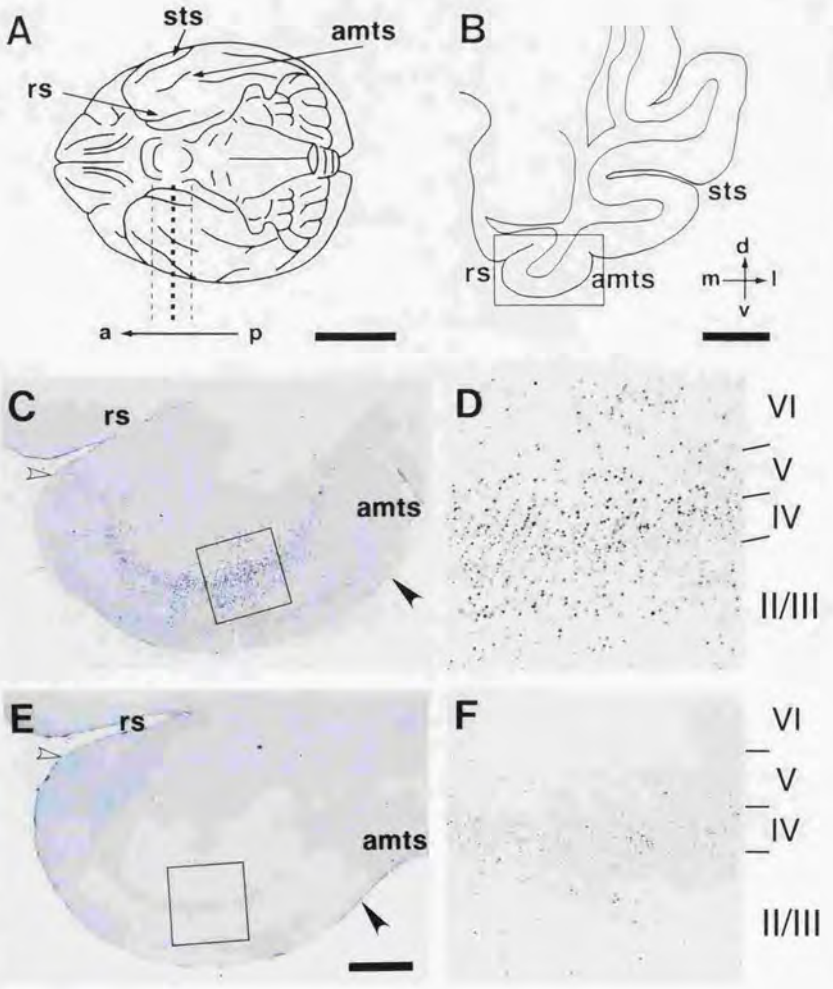
A
sts
amts
rs
a
p
B
sts
rs
amts
d
m
l
v
C
rs
amts
D
VI
V
IV
II/III
E
rs
amts
F
VI
V
IV
II/III

Figure 8

visual paired associate learning was prominent in area 36. By contrast, in area 35 that is medially adjacent to area 36, Zif268 expression levels were low during both types of visual learning.

Legends

Fig. 8. Expression of Zif268 in the monkey inferior temporal gyrus. (A and B) Line drawings of monkey brain (ventral view, A) and of coronal section of the temporal lobe (B). A thick dashed line in A indicates the anterior-posterior level of the coronal section shown in B and thin dashed lines indicate the borders of the area unfolded in the map in Fig 10. The framed area in B is shown in C. Orientation is indicated by arrows: a, anterior; p, posterior; d, dorsal; v, ventral; m, medial; l, lateral. *rs*, rhinal sulcus; *amts*, anterior middle temporal sulcus; *sts*, superior temporal sulcus. Scale bars, 20 mm in A and 5 mm in B. (C-F) Zif268-immunostained sections of the inferior temporal gyrus. A representative Zif268-immunostained section of the monkey inferior temporal gyrus during visual paired associate learning (C). The corresponding section of the monkey with visual discrimination learning is shown in E. Filled and open arrowheads indicate the boundaries between areas 36 and TE and between areas 35 and 36, respectively. Framed areas in C and E are expanded and shown in D and F, respectively. The cortical layers identified in adjacent sections stained with cresyl violet are indicated with Roman numerals in D and F. Scale bar, 1 mm.

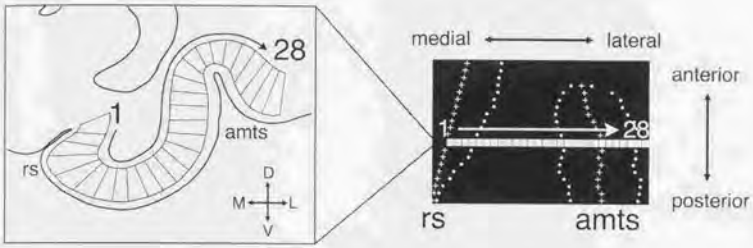

Fig. 9. Two-dimensional unfolded maps of the monkey temporal cortex. The cortical area in each section was subdivided into a number of radial segments (left). To display the spatial distribution of the Zif268 expression levels, the segmented areas were reconstructed into a two-dimensional unfolded map (right). The fundus and lip of a sulcus are outlined by white crosses and white dots, respectively. Serial sections were aligned along the fundus of the rhinal sulcus. rs, rhinal sulcus; amts, anterior middle temporal sulcus.

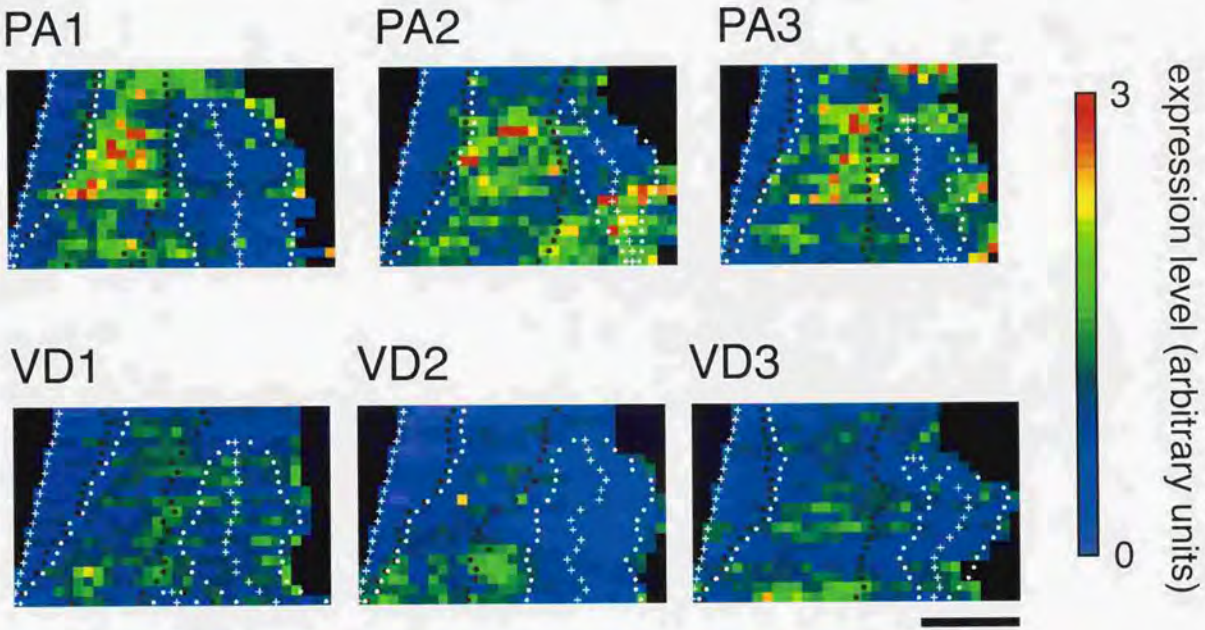

Figure 10

Legends

Fig. 10. The expression levels of Zif268 in the temporal cortex of individual monkeys. The density of reaction products of Zif268-immunostaining in the segments is indicated on the unfolded maps (similar to the right panel in A) in pseudocolor representation. The maps from monkeys with visual paired associate learning (PA1-PA3) and visual discrimination learning (VD1-VD3) are shown in upper panels and lower panels, respectively. The boundaries of cortical areas were indicated by gray dots. The values (arbitrary units; see Methods) are normalized so that the mean density of the reaction products of all segments from all six monkeys is 1.0. Scale bar, 10 mm.

Expression of Zif268 in the hippocampal formation

I next compared the expression of Zif268 in the hippocampal formation including the hippocampus, dentate gyrus and entorhinal cortex between visual paired associate learning and visual discrimination learning groups (Fig. 11). In the dentate gyrus, most granule cells did not express Zif268 (Fig. 11C, H). In the hippocampus, moderately stained Zif268-immunopositive neurons were found in the pyramidal cell layer in both monkey groups. No difference in the Zif268 expression level was observed between the two monkey groups (Fig. 11D, I). Likewise, the expression levels of Zif268 in the entorhinal cortex were similar between the two monkey groups (Fig. 11E, J). These expression patterns of Zif268 in the hippocampal formation were similar to those in non-task-performing (naive) monkeys reported previously (Okuno *et al.*, 1995).

Legends

Fig. 11. Expression of Zif268 in the monkey hippocampal formation. (A) A line drawing of a representative coronal section containing the dentate gyrus, hippocampus and entorhinal cortex. The framed areas are shown in B and F. rs, rhinal sulcus; amts, anterior middle temporal sulcus. (B-E) The hippocampus and dentate gyrus (B), and the entorhinal cortex (E) in the Zif268-immunostained section of the monkey with visual paired associate learning. The framed areas in A are shown in B and E, and the framed areas in B are expanded and shown in C (dentate gyrus) and D (hippocampus, CA1). (F-J) Similar to A-E but in the monkey with visual discrimination learning. The framed areas in F are shown in G and J and the framed areas in G are expanded and shown in H and I. Scale bars, 5 mm in F; 0.5 mm in G; 200μm in H; 0.5 mm in J.

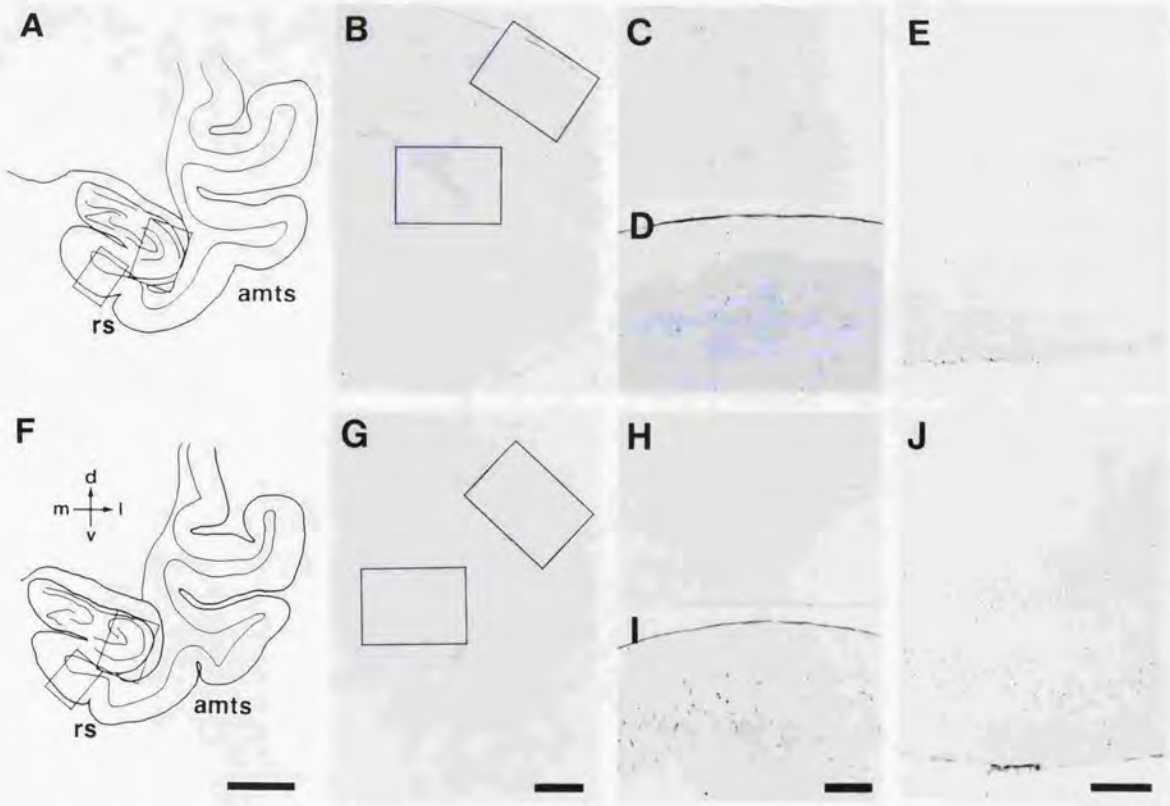

Figure 11

Expression of other transcription factors encoded by IEGs

I further examined whether other IEGs were expressed in the monkey temporal lobe. Transcription factors, Fos and Jun families as well as Zif268 are induced in the rodent hippocampal formation and related cortex after electrical stimulation or convulsant administration (Morgan and Curran., 1991). In the sections immunostained with an anti-c-Fos antibody, I failed to detect immunopositive cells in the inferior temporal cortex and hippocampal formation in either monkey group (data not shown). However, I cannot exclude the possibility that the antibody might be too weakly cross-reactive to monkey c-Fos, although the antigen for the antibody is conserved among rodents and humans and I have positive controls for my c-Fos immunohistochemistry using rat brains treated with electrical stimulation or convulsant.

One of the Jun family proteins, JunD, is expressed in several areas of the monkey cerebral cortex at moderate levels (Okuno *et al.*, 1997). In the temporal cortex including the inferior temporal gyrus, JunD-immunopositive cells were observed in the monkeys with both visual paired associate learning and visual discrimination learning (Fig. 12A, D). In contrast to that of Zif268, the distribution of the JunD-immunopositive cells was rather homogeneous, even in the sections adjacent to the Zif268-immunostained sections that showed patchy expression of Zif268, and no difference in the distribution of JunD-immunopositive cells was observed between the two monkey groups. In the hippocampal formation, JunD-immunopositive cells were also observed in the hippocampus, dentate gyrus and entorhinal cortex, but there was no difference between the two monkey groups (Fig. 12B, C, E, F).

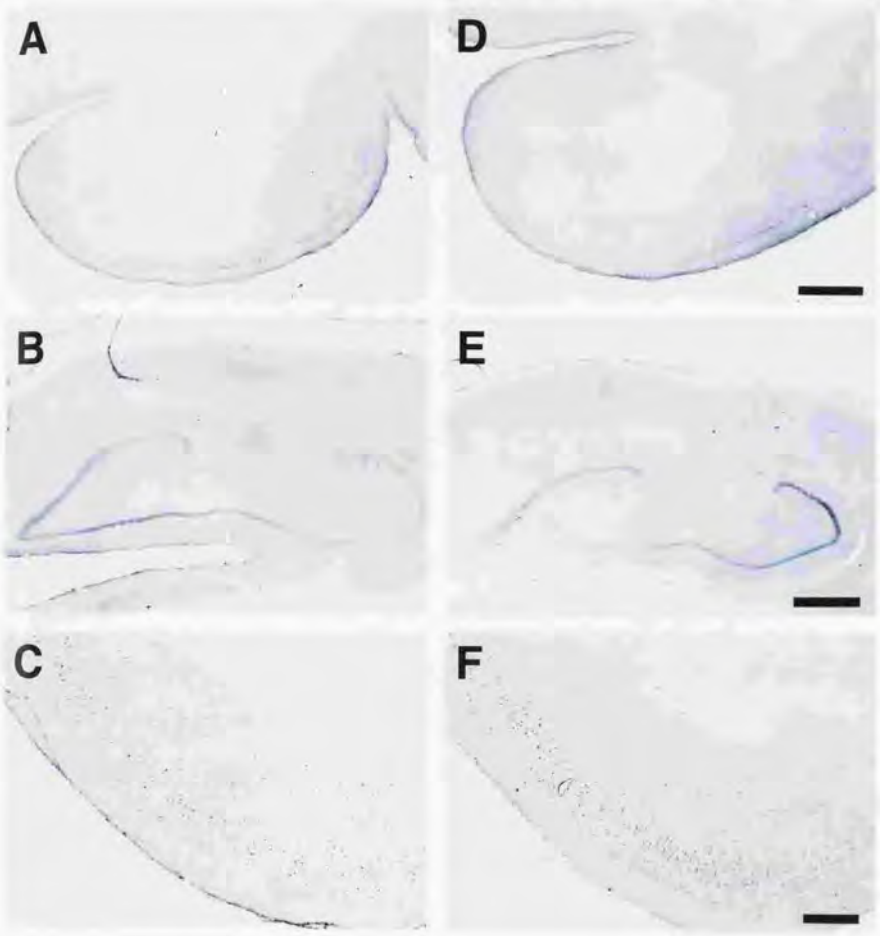

Fig. 12. Expression of JunD in the inferior temporal gyrus and the hippocampal formation. (A-C) Representative JunD-immunostained sections during visual paired associate learning. (A) the inferior temporal gyrus; (B) the hippocampus and dentate gyrus; (C) the entorhinal cortex. (D and F) Similar to A to C but in the monkey with visual discrimination learning. Scale bar, 1 mm in D and E; 0.5 mm in F.

Quantitative comparison of zif268 mRNA expression levels

Finally, I investigated quantitative difference in *zif*268 mRNA expression levels in area 36 during the visual paired associate learning and the visual discrimination learning (Fig. 13). I used split-brain animals to circumvent animal-to-animal variation in mRNA expression levels. Before the start of behavioral training, monkeys were subjected to the forebrain commissurotomy. I then trained the monkeys to learn both the pair-association task and the visual discrimination task under parafoveal stimulus presentation condition: in task trials, the monkeys were given visual stimuli in one visual hemifield for the pair-association task and in the other hemifield for the discrimination task. This stimulus configuration enables each of the monkeys to perform separately the pair-association task using one hemisphere (PA hemisphere) and the discrimination task using the other (VD hemisphere). After the learning of both tasks in the *training set* of the visual stimuli, monkeys were trained with the *test set* as the case of the immunohistochemical experiments. Before the monkeys' performance reached a plateau level, their brains were removed and the total RNA was extracted from visual and vision-related areas.

The RNA samples were analyzed by an RT-PCR-based quantitative method based on coamplification of a target gene with an endogenous internal standard gene (Okuno *et al.*, 1999). In the RT-PCR coamplification method, the reverse-transcribed mRNA of the target gene was simultaneously amplified with that of an internal standard gene in the same reaction tube. By normalization with the quantity of the internal standard gene product, the relative mRNA expression levels of the target gene could be compared across hemispheres. I have performed several control experiments to check fidelity of this RT-PCR coamplification method. I first confirmed the absence of interference in the PCR amplification of the target and the internal standard (Fig. 13B, upper panel). Total RNA extracted from the monkey

cerebral cortex were reverse-transcribed followed by PCR amplification using two sets of primers, one for the *zif*268 gene and the other for an endogenous internal standard gene, the G6PD gene. Two fragments were specifically amplified in a cycle-dependent manner. The sizes (250 bp, upper band; 211 bp, lower band) were identical to those of *zif*268 and G6PD fragments observed under the single-gene amplification conditions, indicating no interference between the primers. I next examined the cycle-dependency of amplification efficiency under the coamplification conditions in order to determine the range of the exponential amplification phase (Fig. 13B, lower panel). During 15 to 19 PCR cycles, the amplification rates deduced from the slopes of the regression lines ranged from 1.97 to 1.99 per PCR cycle, which indicate the target and internal standard genes were coamplified with the same efficiency. I finally confirmed the range of template amounts for faithful quantification. At the PCR cycles 15 to 19, there is a linear relationship between amplified product amounts and template amounts at the range of 0.01 to 1 atto-mol templates per reaction tube (Okuno *et al.*, in preparation), indicating that no "plateau" effects occur in my RT-PCR coamplification experiments.

By using this coamplification method, I quantified *zif*268 mRNA expression levels in various cortical areas during the learning of visual memory tasks in individual animals (Fig. 14). Figure 14A shows representative autoradiographic patterns demonstrating *zif*268 mRNA expression in the PA and VD hemispheres. The RNA sample extracted from area 36 of the PA hemisphere yielded an intense *zif*268 band compared to that of the VD hemisphere. By contrast, the intensities of *zif*268 bands did not appear to be different between the hemispheres in other cortical areas, primary visual area V1, visual association area TE and the hippocampus. The intensities of the G6PD bands were relatively constant between the hemispheres in each cortical area. I measured the amounts of these bands using independent

RNA samples from five monkeys, and the *zif*268 mRNA expression levels were normalized by that of the internal standard gene (Fig. 14B). In area 36, the *zif*268 expression level in the PA hemisphere was significantly higher than that in the VD hemisphere ($P < 0.05$, paired *t*-test, $d.f. = 4$). There were no statistical differences in the *zif*268 mRNA levels between the hemisphere in other cortical area. I finally calculated the ratio of *zif*268 mRNA expression levels in the PA hemisphere to that in the VD hemisphere in each animal, and the ratios were then averaged across animals (Fig. 14C). This intra-animal comparison revealed that the *zif*268 expression levels in the PA hemisphere were approximately 1.25-fold higher than that in the VD hemisphere, and is statistically different from theoretical ratio of 1.00 when the expression levels are the same between the hemispheres ($P < 0.05$, $d.f. = 4$).

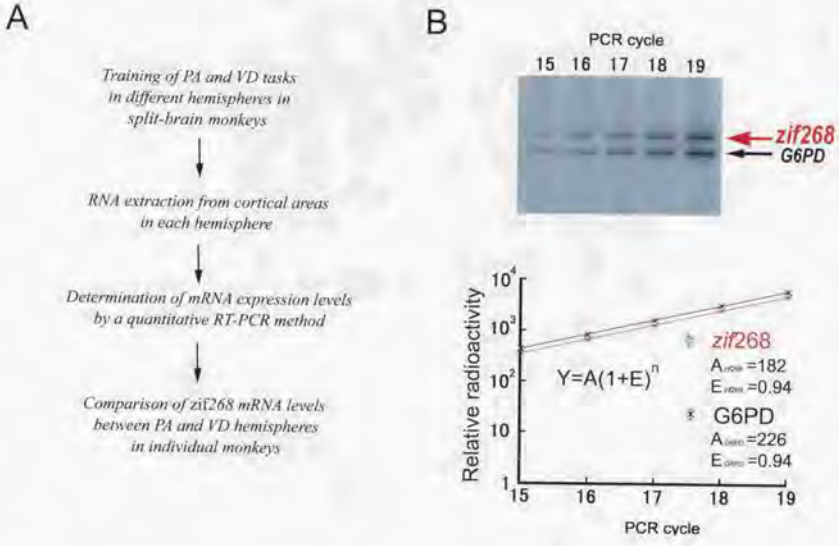

Fig. 13 Quantification of the *zif*268 mRNA expression levels in different memory tasks. (A) Experimental flow for mRNA quantification. Macaque monkeys that underwent forebrain commissurotomy were trained in two different tasks under the lateralized stimulus presentation condition. Each of monkeys separately used one hemisphere to perform the pair-association (PA) task and the other hemisphere to perform the visual discrimination (VD) task. Before the monkeys' performance reached a plateau level, their brains were removed and the total RNA was extracted from various cortical areas. The mRNA expression level of *zif*268 in each cortical area was quantified by a quantitative RT-PCR method, and the expression levels were compared across PA and VD hemispheres. (B) PCR coamplification of target and internal standard genes in single reaction tubes. Total RNA was reverse-transcribed followed by PCR coamplification by using the primers for the monkey *zif*268 and G6PD genes (upper panel). The radioactivity of PCR products was quantitated by using an image analyzer, and logarithmically plotted against PCR cycles (lower panel). The data represent mean of three independent experiments. Red and black lines indicate regression lines fit to the data points for *zif*268 and G6PD, respectively ($R^2 = 0.999$ for both *zif*268 and G6PD).

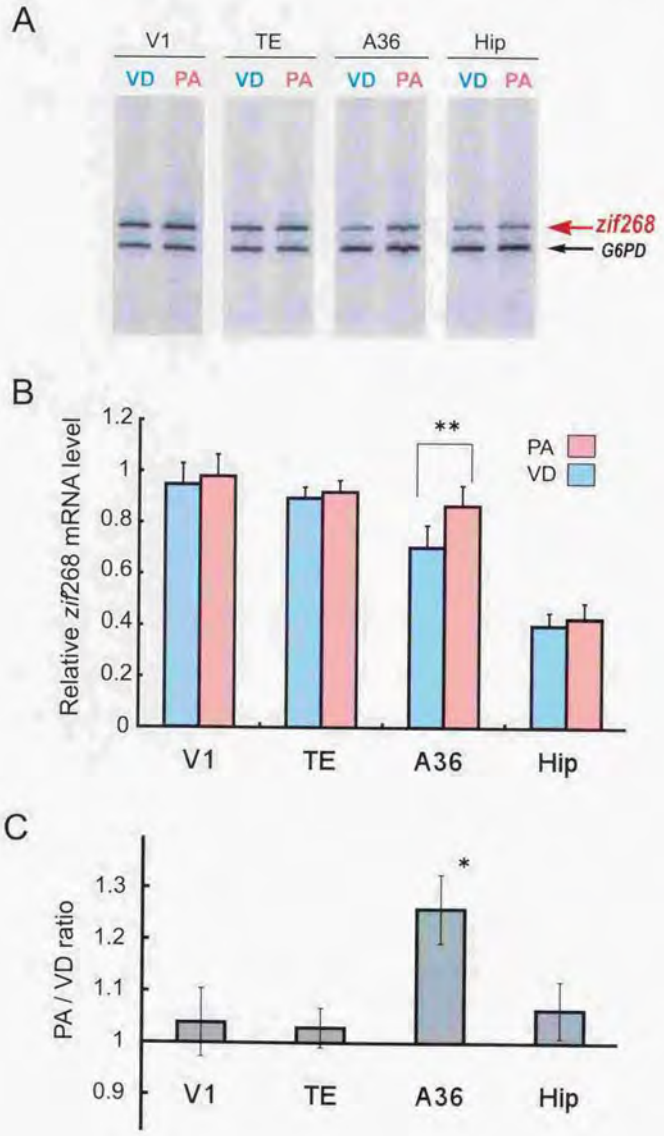
A
V1
TE
A36
Hip
VD PA VD PA VD PA VD PA
zif268
G6PD
B
Relative zif268 mRNA level
1.2
1
0.8
0.6
0.4
0.2
0
**
PA
VD
V1
TE
A36
Hip
C
PA / VD ratio
1.3
1.2
1.1
1
0.9
*
V1
TE
A36
Hip

Figure 14

Legends

Fig. 14. Comparison of *zif*268 mRNA expression levels during PA and VD learning. (A) Representative autoradiographic patterns in the *zif*268 mRNA quantification. Total RNAs extracted from the PA and VD hemispheres in each monkey were analyzed by the PCR coamplification method. V1, the primary visual cortex; TE, unimodal visual area TE in the temporal association cortex; A36, area 36 in the perirhinal cortex; Hip, the hippocampus. (B) The relative *zif*268 mRNA expression levels in the PA and VD hemisphere. For normalization, the radioactivity of *zif*268 band was divided by that of the internal standard band, and the relative *zif*268 mRNA levels were averaged across animals (N=5; error bar, s.e.m) in each hemisphere and each cortical area. The mean *zif*268 expression levels in area 36 were significantly higher in PA hemisphere than in VD hemisphere (**, $P < 0.01$, paired *t*-test). There was no statistical difference in the *zif*268 expression levels in other cortical areas. (C) Ratio of *zif*268 expression levels in the PA hemisphere to that in the VD hemisphere. For each animal, the relative *zif*268 mRNA levels in the PA hemisphere was divided by that in the VD hemisphere in each cortical area. The ratios were then averaged across animals (error bar, s.e.m). The ratio in area 36 is significantly higher than one (*, $P < 0.05$, *t*-test).

DISCUSSION

Gene expression in the monkey perirhinal cortex

This is the first report regarding the gene expression changes during long-term memory formation in the primate. I detected the altered expression of both Zif268 protein and *zif*268 mRNA in the monkey perirhinal cortex, area 36, during visual paired associate learning compared with during visual discrimination learning. During visual paired associate learning, Zif268-immunopositive neurons were accumulated in patches that spread into superficial and deep layers in the inferior temporal gyrus (Fig. 8C, D). High-level expression of Zif268 was localized in a strip along the rhinal sulcus (Fig. 10). In contrast to the strong patchy expression of Zif268, the expression of other IEG products did not show such patterns (Fig. 6). JunD-immunopositive cells were distributed homogeneously in the inferior temporal gyrus (Fig. 12A, D). These results suggest that Zif268 is most efficiently induced among transcription factors encoded by IEGs in the anterior temporal lobe under this condition. I further quantitatively compared the *zif*268 mRNA expression levels during the paired associate and discrimination learning. I found that, in area 36, the *zif*268 mRNA levels during the paired associate learning were significantly higher than that during the discrimination learning (Fig. 14).

It was revealed by tracer experiments that the anterior part of the monkey inferior temporal gyrus was organized into several bands which extended along the rhinal sulcus in an anterior-posterior axis and which received afferents from specific areas of the anterior part of the middle temporal gyrus and the posterior part of the inferior temporal gyrus (Martin-Elkins and Horel, 1992). This organization might contribute to the strip-like expression of Zif268 observed in this study.

The monkey inferior temporal gyrus consists of the perirhinal cortex (area 35 and area 36) and ventral part of unimodal visual association area TE (Insausti *et al.*, 1987; Martin-Elkins and Horel, 1992). The perirhinal cortex, especially area 36, receives strong visual input from various cortical areas (Van Essen *et al.*, 1992; Murray and Bussey, 1999). Area 36 sends projections, directly or indirectly through area 35, to the entorhinal cortex and the hippocampus (Suzuki and Amaral, 1994; Suzuki 1996). These neural circuits are proposed to be important for memory formation, especially in vision (Mishkin, 1982; Squire and Zola-Morgan, 1991; Miyashita, 1993). The anterior temporal cortex including area 36 contains visual memory neurons that selectively responded to both pictures of the paired associates and that reflected presumably memory storage elements between the paired associates (Sakai and Miyashita, 1991; Miyashita *et al.*, 1993). It was also reported that disruption of the backward projection from the perirhinal/entorhinal cortex to the inferior temporal cortex (IT) abolished formation of the associative codes in IT neurons (Higuchi and Miyashita, 1996). From these previous findings with the results in the present study, I propose a hypothesis that the gene activation in area 36 contributes to neuronal reorganization underlying the formation and maintenance of long-term memory for visual stimulus-stimulus associations (Fig. 15).

Task-dependent gene expression in the perirhinal cortex

In this study, I used visual discrimination learning as a control for visual paired associate learning because, under no task condition, it was difficult to regulate the mental activity related to memory formation, or even to regulate the motor activity in the monkeys. The difference in both Zif268 expression patterns and *zif*268 mRNA levels between visual paired associate learning and visual discrimination learning most likely originated from differences in neuronal activities related to memory requirements of the two tasks, for several reasons.

First, the experimental conditions were almost identical between the two tasks, i.e., the same task apparatus with the same touch sensor, the same visual stimuli and the same reward were used, suggesting that the differential gene expression of *zif*268 was not related to general motor or sensory activity. Second, in RNA quantification experiments, the *zif*268 mRNA expression levels in unimodal visual areas, V1 and TE, were almost the same between two different task conditions. These results indicate that the difference was not associated with the amount of sensory input. Also, Zif268 expression patterns in the entorhinal cortex or in the hippocampus were almost the same between the two monkey groups, confirming the reproducibility of immunostaining among different sections and monkeys. Finally, my results were consistent with those of recent behavioral studies. Ablations of the perirhinal/entorhinal cortex cause impairment in learning of visual paired associates (Murray *et al.*, 1993), but not in visual pattern discrimination, even when the lesions were combined with other medial temporal areas (Zola-Morgan *et al.*, 1989, 1993; Suzuki *et al.*, 1993).

The difference in *zif*268 expression between visual paired associate learning and visual discrimination learning might also depend on learning stages as well as the memory requirements of the tasks. Since the visual discrimination task is easier than the visual pair-association task, the monkeys' performance in the visual discrimination task reached a plateau level more quickly (Fig. 5). It is tempting to test a prediction that, even in the visual pair-association task, Zif268 would not be expressed in an "overtrained" stage.

Roles of IEG expression for memory formation

Although it is not yet well characterized in the mammalian brain, studies in both invertebrates and vertebrates have revealed that formation of long-term memory requires new protein and mRNA synthesis whereas formation of short-term memory does not (Bailey and Kandel,

1993; Tully *et al.*, 1994). The requirement of *de novo* protein and mRNA synthesis for long-term memory suggests that neuronal activities induced by learning initiate a cascade of gene expression. The first step of the gene cascade is thought to be expressions of IEGs. Transcription factors encoded by IEGs have been proposed to play a role in the establishment of long-term changes in the properties of synapses (Sheng and Greenberg, 1990; Morgan and Curran, 1991; Abraham *et al.*, 1993; O'Donovan *et al.*, 1999). The induced transcription factors regulate expression of late-response genes that probably contribute to the synaptic plasticity, especially morphological changes. For example, synapsin-I and neurofilament-light genes are activated by Zif268 (Pospelov *et al.*, 1994; Thiel *et al.*, 1994). Moreover, many IEGs including *zif*268 have cyclic AMP responsive element (CRE) sequences in their promoter regions and their expression can be controlled by CRE-binding proteins (CREBs) (Vaccarino *et al.*, 1993; Sakamoto *et al.*, 1994). Lines of studies have shown CREB involvement in the formation and consolidation of various classes of long-term memory in several species (Dash *et al.*, 1990; Bourtchuladze *et al.*, 1994; Yin *et al.*, 1994). Taken together, the expression of Zif268 in the temporal cortex observed in this study suggest that *zif*268 expression in area 36 may participate in the gene cascade related to formation and maintenance of visual associative memory in the primate.

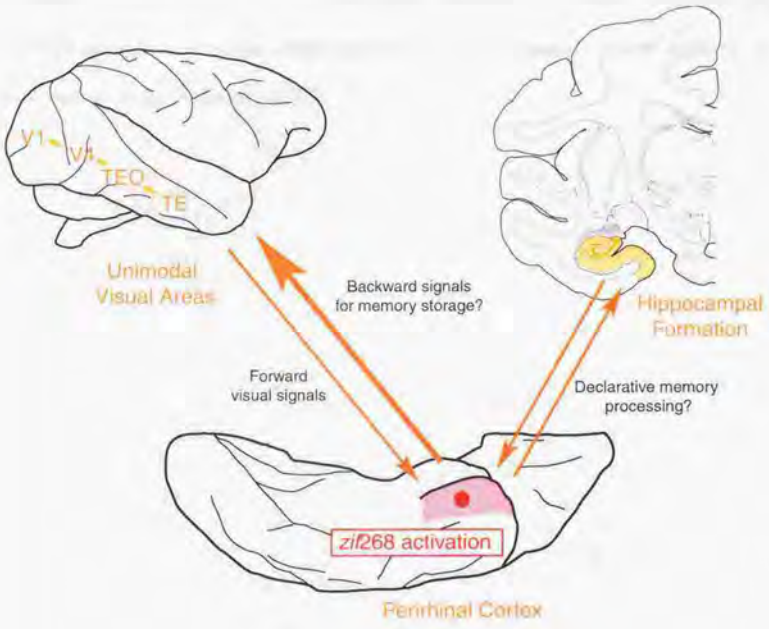

Fig. 15. A possible role of gene activation in the perirhinal cortex during paired associate learning. The gene activation in the perirhinal cortex may induce neuronal reorganization in the backward connections from the perirhinal cortex to the temporal association areas. Other connections, such as forward projections from the temporal visual areas or reciprocal connections with the hippocampal formation, may also alter after the gene activation in the perirhinal cortex.

ACKNOWLEDGMENTS

I am sincerely grateful to Professor Yasushi Miyashita for valuable discussions and continuous supports during the course of this study. I thank Dr. D. Saffen for providing the anti-Zif268 antibody, for helpful advice and for his encouragement. I also thank Dr. C. Hamada for advice on statistical analysis.

REFERENCES

Abraham, W. C., Mason, S. E., Demmer, J., Williams, J. M., Richardson, C. L., Tate, W. P., Lawlor, P. A. and Dragunow, M. (1993) Correlations between immediate early gene induction and the persistence of long-term potentiation. *Neuroscience*, **56,** 717-727.

Abraham, W. C., Christie, B. R., Logan, B., Lawlor, P. and Dragunow, M. (1994) Immediate early gene expression associated with the persistence of heterosynaptic long-term depression in the hippocampus. *Proc. Natl. Acad. Sci. USA*, **91,** 10049-10053.

Alberini, C. M., Ghirardi, M., Metz, R. and Kandel, E. R. (1994) C/EBP is an immediate early gene required for the consolidation of long-term facilitation in Aplysia. *Cell*, **76,** 1099-1114.

Amaral, D. G., Insausti, R. and Cowan, W. M. (1987) The entorhinal cortex of the monkey: I. Cytoarchitectonic organization. *J. Comp. Neurol.*, **264,** 326-355.

Bailey, C. H. and Kandel, E. R. (1993) Structural changes accompanying memory storage. *Annu. Rev. Physiol.*, **55,** 397-426.

Baum, M. J. and Everitt, B. J. (1992) Increased expression of c-*fos* in the medial preoptic area after mating in the male rat: role of afferent inputs from the medial amygdala and midbrain central tegmental field. *Neuroscience*, **50,** 627-646.

Bito, H., Deisseroth, K. and Tsien R. W. (1996) CREB phosphorylation and dephosphorylation: a Ca^{2+}- and stimulus duration-dependent switch for hippocampal gene expression. *Cell.* **87,** 1203-1214.

Bourtchuladze, R., Frenguelli, B., Blendy, J., Cioffi, D., Schultz, G. and Silva, A. J. (1994) Deficient long-term memory in mice with a targeted mutation of the cAMP-responsive element-binding protein. *Cell.* **79,** 59-68.

Changelian, P. S., Feng, P., King, T. C. and Milbrandt, J. (1989) Structure of the NGFI-A gene and detection of upstream sequences responsible for the its transcriptional induction by nerve growth factor. *Proc. Natl. Acad. Sci. USA.* **86,** 377-381.

Chaudhuri, A., Matubara, J. A. and Cynader, M. S. (1995) Neuronal activity in primate visual cortex assessed by immunostaining for the transcription factor Zif268. *Vis. Neurosci.*, **12,** 35-50.

Chelly, J., Kaplan, J. C., Maire, P., Gautron, S. and Kahn A. (1988) Transcription of the dystrophin gene in human muscle and non-muscle tissue. *Nature,* **333,** 858-860.

Christy B. and Nathans, D. (1989) Functional serum responsive elements upstream of the growth factor-inducible gene zif268. *Mol. Cell. Biol.*, **9,** 4889-4995.

Cole, A. J., Saffen, D. W., Baraban, J. M. and Worley, P. F. (1989) Rapid increase of an immediate early gene messenger RNA in hippocampal neurons by synaptic NMDA receptor activation *Nature,* **340,** 474-476.

Cole, A. J., Abu-Shakra, S., Saffen, D. W., Baraban, J. M. and Worley, P. F. (1990) Rapid rise in transcription factor mRNAs in rat brain after electroshock-induced seizures. *J. Neurochem.,* **55,** 1920-1927.

Cole, A. J., Bhat, R. V., Patt, C., Worley, P. F. and Baraban, J. M. (1992) D1 dopamine receptor activation of multiple transcription factor genes in rat striatum. *J. Neurochem.,* **58,** 1420-1426.

Dash, P. K., Hochner, B. and Kandel, E. R. (1990) Injection of the cAMP-responsive element into the nucleus of Aplysia sensory neurons blocks long-term facilitation. *Nature,* **345,** 718-721.

Ebihara, T. and Saffen, D. (1997) Muscarinic acetylcholine receptor-mediated induction of *zif*268 mRNA in PC12D cells requires protein kinase C and the influx of extra ellular calcium. *J. Neurochem.,* **68,** 1001-1010.

Gause, W. C. and Adamovicz J. (1995) Use of PCR to quantitate relative differences in gene expression. In C.W. Dieffenbach and G.S. Dveksler (eds): *PCR primer: a laboratory manual.* New York: Cold Spring Harbor Lab. Press, pp. 293-311.

Ginty, D. D., Glowacka, D., Bader, D. S., Hidaka, H. and Wagner J. A. (1991) Induction of immediate early genes by Ca^{2+} influx requires cAMP-dependent protein kinase in PC12 cells. *J. Biol. Chem.*, **266,** 17454-17458.

Ginty, D.D., Bading, H. and Greenberg, M.E. (1992) Trans-synaptic regulation of gene expression. *Curr. Opin. Neurobiol.*, **2,** 312-316.

Hasegawa, I., Fukushima, T., Ihara, T. and Miyashita, Y. (1998) Callosal window between prefrontal cortices: cognitive interaction to retrieve long-term memory. *Science*, **281,** 814-818.

Herdegen, T., Sandkuhler, J., Gass, P., Kiessling, M., Bravo, R. and Zimmermann, M. (1993) JUN, FOS, KROX, and CREB transcription factor proteins in the rat cortex: Basal expression and induction by spreading depression and epileptic seizures. *J. Comp. Neurol.*, **333,** 271-288.

Higuchi, S. and Miyashita, Y. (1996) Formation of mnemonic neuronal responses to visual paired associates in inferotemporal cortex is impaired by perirhinal and entorhinal lesions. *Proc. Natl. Acad. Sci. USA*, **93,** 739-743.

Hill, C. S. and Treisman R. (1995) Transcriptional regulation by extracellular signals: mechanisms and specificity. *Cell*, **80,** 199-211.

Horel, J. A., Pytko-Joiner, D. E., Voytko, M. L. and Salsbury, K. (1987) The performance of visual tasks while segments of the inferotemporal cortex are suppressed by cold. *Behav. Brain Res.*, **23,** 29-42.

Hughes, P. and Dragunow, M. (1995) Induction of immediate-early genes and the control of neurotransmitter-regulated gene expression within the nervous system. *Pharmacol. Reviews*, **47,** 133-178.

Hughes, P., Beilharz, E., Gluckman, P. and Dragunow, M. (1993) Brain-derived neurotrophic factor is induced as an immediate early gene following *N*-methyl-*D*-aspartate receptor activation. *Neuroscience*, **57,** 319-328.

Insausti, R., Amaral, D. G. and Cowan, W. M. (1987) The entorhinal cortex of the monkey: II. Cortical afferents. *J. Comp. Neurol.*, **264,** 356-395.

Iwai, E. and Mishkin, M. (1969) Further evidence on the locus of the visual area in the temporal lobe of the monkey. *Exp. Neurol.*, **25,** 585-594.

Iwai, E., Yukie, M., Suyama, H. and Shirakawa S. (1987) Amygdalar connections with middle and inferior temporal gyri of the monkey. *Neurosci. lett.*, **83**, 25-29.

Jarvis, E. D., Mello, C. V. and Nottebohm, F. (1995) Associative learning and stimulus novelty influence the song-induced expression of an immediate early gene in the canary forebrain. *Learn. Mem.*, **2,** 62-80.

Kumahara, E., Ebihara, T. and Saffen, D. (1999) Protein kinase inhibitor H7 blocks the induction of immediate-early genes *zif*268 and c-*fos* by a mechanism unrelated to inhibition of protein kinase C but possibly related to inhibition of phosphorylation of RNA polymerase II. *J. Biol. Chem.*, **274,** 10430-10438.

Lemaire, P., Revelant, R., Bravo, R. and Charnay, P. (1988) Two mouse genes encoding potential transcription factors with identical DNA-binding domains are activated by growth factors in cultured cells. *Proc. Natl. Acad. Sci. USA,* **85,** 4691-4695.

Lerea, L. S., Butler, L. S. and McNamra J. O. (1992) NMDA and non-NMDA receptor-mediated increase of c-*fos* mRNA in dentate gyrus neurons involves calcium influx via different routes. *J.Neurosci.* **12,** 2973-2981.

Lund, J. S. (1988) Anatomical organization of macaque monkey striate visual cortex. *Annu.Rev.Neurosci.* **11,** 253-288.

Mack, K. J. and Mack, P. A. (1992) Induction of transcription factor in somatosensory cortex after tactile stimulation. *Mol. Brain Res.*, **12,** 141-147.

Marshall, C. J. (1995) Specificity of receptor tyrosine kinase signaling: transient versus sustained extracellular signal-regulated kinase activation. *Cell,* **80,** 107-121.

Martin-Elkins, C. L. and Horel, J. A. (1992) Cortical afferents to behaviorally defined regions of the inferior temporal and parahippocampal gyri as demonstrated by WGA-HRP. *J. Comp. Neurol.*, **321,** 177-192.

McMahon, S. B. and Monroe, J. G. (1995) A ternary complex factor-dependent mechanisms mediates induction of *egr*-1 through selective serum response elements following antigene receptor cross-linking in B lymphocytes. *Mol. Cell. Biol.*. **15,** 1086-1093.

Mello, C. V., Vicario, D. S. and Clayton, D. F. (1992) Song presentation induces gene expression in the song bird forebrain. *Proc. Natl. Acad. Sci. USA.* **89,** 6818-6822.

Mishkin, M. (1982) A memory system in the monkey. *Phil. Trans. R. Soc. Lond. [Biol.].* **298,** 85-95.

Miyashita, Y. (1993) Inferior temporal cortex: Where visual perception meets memory. *Annu. Rev. Neurosci.*. **16,** 245-263.

Miyashita, Y., Date, A. and Okuno, H. (1993) Configuration encoding of complex visual forms by single neurons of monkey temporal cortex. *Neuropsychologia.* **31,** 1119-1131.

Morgan, J. I. and Curran, T. (1991) Stimulus-transcription coupling in the nervous system: Involvement of the inducible proto-oncogenes fos and jun. *Annu. Rev. Neurosci.* **14,** 421-451.

Morgan, J. I., Cohen, D. R., Hempstead, J. L. and Curran, T. (1987) Mapping patterns of c-*fos* expression in the central nervous system after seizure. *Science*, **237,** 192-197.

Murray, E. A. and Mishkin, M. (1986) Visual recognition in monkeys following rhinal cortical ablations combined with either amygdalectomy or hippocampectomy. *J. Neurosci.*, **6,** 1991-2003.

Murray, E. A. and Bussey, T. J. (1999) Perceptual-mnemonic functions of the perirhinal cortex. *Trends Cogn. Sci.*, **3,** 142-151.

Murray, E. A., Gaffan, D. and Mishkin, M. (1993) Neural substrates of visual stimulus-stimulus association in rhesus monkeys. *J. Neurosci.*, **13,** 4549-4541.

O'Donovan, K. J., Tourtellotte, W. G., Milbrandt, J. and Baraban, J. M. (1999) The EGR family of transcription-regulatory factors: progress at the interface of molecular and system neuroscience. *Trends Neurosci.*, **22,** 167-173.

Okuno, H., Suzuki, T., Hashimoto, Y., Curran, T. and Iba, H. (1991) Inhibition of jun transformation by a mutated fos gene: design of an anti-oncogene. *Oncogene*, **6,** 1491-1497.

Okuno, H., Akahori, A., Sato, H., Xanthoudakis, S., Curran, T. and Iba, H. (1993) Escape from redox regulation enhances the transforming activity of Fos. *Oncogene*, **8,** 695-701.

Okuno, H., Saffen, D. W. and Miyashita, Y. (1995) Subdivision-specific expression of Zif268 in the hippocampal formation of the Macaque monkey. *Neuroscience.* **66,** 829-845.

Okuno, H., Kanou, S., Tokuyama, W., Li, Y-X. and Miyashita, Y. (1997) Layer-specific differential regulation of transcription factors Zif268 and JunD in visual cortex V1 and V2 of macaque monkeys. *Neuroscience* **81,** 653-666.

Okuno, H., Tokuyama, W., Li, Y-X., Hashimoto, T. and Miyashita, Y. (1999) Quantitative evaluation of neurotrophin and *trk* mRNA expression in visual and limbic areas along the occipito-temporo-hippocampal pathway in adult macaque monkeys. *J. Comp. Neurol.* **408,** 378-398.

Pang, S., Koyanagi, Y., Miles, S., Wiley, C., Vinters, H.V., and Chen, I.S. (1990) High levels of unintegrated HIV-1 DNA in brain tissue of AIDS dementia patients. *Nature.* **343,** 85-89.

Pospelov, V. A., Pospelova, T. V. and Julien, J. P. (1994) AP-1 and Krox-24 transcription factors activate the neurofilament light gene promoter in P19 embryonal carcinoma cells. *Cell Growth Differ.*, **5,** 187-196.

Rosen, K. M., McCormack, M. A., Villa-Komaroff, L. and Mower, G. D. (1992) Brief visual experience induces immediate early gene expression in the cat visual cortex. *Proc. Natl. Acad. Sci. USA.* **89,** 5437-5441.

Saffen, D. W., Cole, A. J., Worley, P. F., Christy, B. A., Ryder, K. and Baraban, J. M. (1988) Convulsant-induced increase in transcription factor messenger RNAs in rat brain. *Proc. Natl. Acad. Sci. USA*, **85,** 7795-7799.

Sakai, K. and Miyashita, Y. (1991) Neural organization for the long-term memory of paired associates. *Nature*, **354,** 152-155.

Sakamoto, K. M., Fraser, J. K., Lee, H., J., Lehman, E. and Gasson, J. C. (1994) Granulocyte-macrophage colony-stimulating factor and interleukin-3 signaling pathways converge on the CREB-binding site in the human *egr*-1 promoter. *Mol. Cell Biol.*, **14,** 5975-5985.

Sheng, M. and Greenberg, M. E. (1990) The regulation and function of c-*fos* and other immediate early genes in the nervous system. *Neuron*, **4,** 477-485.

Squire, L. R. and Zola-Morgan, S. (1991) The medial temporal lobe memory system. *Science*, **253,** 1380-1386.

Suzuki W. A., (1996) The anatomy, physiology and functions of the perirhinal cortex. *Curr. Opin. Neurobiol.*, **6,** 179-186.

Suzuki, W. A. and Amaral, D. G. (1994) Topographic organization of the reciprocal connections between the monkey entorhinal cortex and the perirhinal and parahippocampal cortices. *J. Neurosci.*, **14,** 1856-1877.

Suzuki, W. A., Zola-Morgan, S., Squire, L. R. and Amaral, D. G. (1993) Lesions of the perirhinal and parahippocampal cortices in the monkey produce long-lasting memory impairment in the visual and tactual modalities. *J. Neurosci.*, **13,** 2430-2451.

Thiel, G., Schoch, S. and Petersohn, D. (1994) Regulation of synapsin I gene expression by the zinc finger transcription factor zif268/egr-1. *J. Biol. Chem.*, **269,** 15294-15301.

Tokuyama, W., Hashimoto, T., Li, Y-X., Okuno, H. and Miyashita, Y., (1998). Highest *trk*B mRNA expression in the entorhinal cortex among hippocampal subregions in the adult rat: contrasting pattern with BDNF mRNA expression. *Mol. Brain Res.*, **62,** 206-215.

Tully, T., Preat, T., Boynton, S. C. and Del Vecchio, M. (1994) Genetic dissection of consolidated memory in Drosophila. *Cell*, **79,** 35-47.

Vaccarino, F. M., Hayward, M. D., Le, H. N., Hartigan, D. J., Duman, R. S. and Nestler, E. J. (1993) Induction of immediate early genes by cyclic AMP in primary cultures of neurons from rat cerebral cortex. *Mol. Brain Res.*, **19,** 76-82.

Van Essen, D. C. and Maunsell, J. H. R. (1980) Two-dimensional maps of the cerebral cortex. *J. Comp. Neurol.*, **191,** 225-281.

Van Essen, D. C., Anderson, C. H. and Felleman, D. J. (1992) Information processing in the primate visual system: An integrated systems perspective. *Science*, **255,** 419-423.

Wechsler, D. (1987) *Wechsler Memory Scale-Revised.* Harcourt Brace Jovanovich, San Antonio. The Psychological Corporation.

Worley, P. F., Christy, B. A., Nakabeppu, Y., Bhat, R. V., Cole, A. J. and Baraban, J. M. (1991) Constitutive expression of *zif*268 in neocortex is regulated by synaptic activity. *Proc. Natl. Acad. Sci. USA.* **88,** 5106-5110.

Worley, P. F., Bhat, R. V., Baraban, J. M., Erickson, C. A., McNaughton, B. L. and Barnes, C. A. (1993) Thresholds for synaptic activation of transcription factors in hippocampus: Correlation with long-term enhancement. *J. Neurosci.,* **13,** 4776-4786.

Yin, J. C. P., Wallach, J. S., Del Vecchio, M., Wilder, E. L., Zhou, H., Quinn, W. G. and Tully, T. (1994) Induction of a dominant negative CREB transgene specifically blocks long-term memory in Drosophila. *Cell,* **79,** 49-58.

Zahn, C. T. and Roskies, R. Z. (1972) Fourier descriptors for plane closed curves. *IEEE Trans. Comput.,* **c-21,** 269-281.

Zola-Morgan, S., Squire, L. R., Amaral, D. G. and Suzuki, W. A. (1989) Lesions of perirhinal and parahippocampal cortex that spare the amygdala and hippocampal formation produce severe memory impairment. *J. Neurosci.,* **9,** 4355-4370.

Zola-Morgan, S., Squire, L. R., Clower, R. P. and Rempel, N. L. (1993) Damage to the perirhinal cortex exacerbates memory impairment following lesions to the hippocampal formation. *J. Neurosci.*, **13**, 251-265.

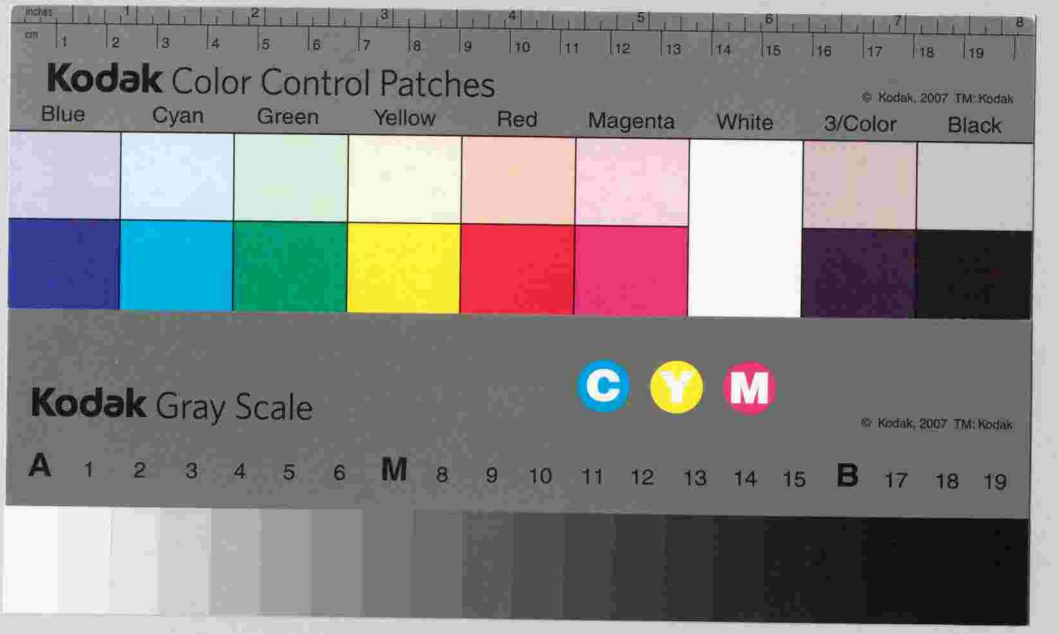
inches
cm
Kodak Color Control Patches
© Kodak, 2007 TM: Kodak
Blue
Cyan
Green
Yellow
Red
Magenta
White
3/Color
Black
Kodak Gray Scale
C
Y
M
© Kodak, 2007 TM: Kodak
A 1 2 3 4 5 6 M 8 9 10 11 12 13 14 15 B 17 18 19